The Effect of the Fractal Guest Subsystem on the Structure, Heat Capacity and Impedance Response of InSe Crystals Intercalated with Nickel

B.O. Seredyuk[1,*], I.I. Grygorchak[2], V.L. Fomenko[3], N.K. Tovstyuk[2]

[1] *National Academy of Land Forces, Faculty of Rocket Troops and Artillery,*
32, Geroiv Majdanu Str., 79012 Lviv, Ukraine
[2] *Lviv Polytechnic National University, 12, Bandera Str., 79000 Lviv, Ukraine*
[3] *Ivan Franko Lviv National University, 50, Dragomanov Str., 79005 Lviv, Ukraine*

The intercalation compounds of Ni_xInSe ($x = 0$; 0.25; 0.5; 0.75; 1.0; 1.25) were produced by the method of direct synthesis of components in quartz ampoules. These compounds are characterized by the formation of discrete nanoislands from the "guest" component as well as their reproduction with the formation of fractal nets. The inductive response at $x = 0.25$, $x = 0.75$, $x = 1.25$, which for the indicated values of x has different intensity and frequency manifestation has been revealed for these structures. An impedance analysis of electrical current passage and its comparison with the data of temperature dependence of electrical conductivity has been carried out. It was found that the linear contribution to the heat capacity from the electrons at the lowest temperatures disappears as a result of intercalation with nickel, and at temperatures below Debye temperature the temperature dependence of the specific heat does not correspond to the expected law of $T^{2 \div 3}$ for the quasi-twodimensional systems. The revealed out of the ordinary effects can be explained by the change in the fractal structure of the clustered nickel guest subsystem.

Keywords: Fractal structure, Intercalation, Inductive response, Heat capacity.

1. INTRODUCTION

Today, the interest of the "guest-host" systems is higher than ever, and not only in connection with incomplete understanding of these processes. So far, practically neither systematic study of the intercalation of materials - "hosts" of the complex molecular structure (with four or more atomic planes in the layer), in general, nor their semiconductor phases with magnetically active components, in particular have been thoroughly studied.

Intercalation, as the process of "constructing" certain types of systems, "guest-host", in addition to the simple broadening of the range of new compounds, can result in enriching the original crystals with unique properties that are not inherent to them. So new technological approaches and specific operations forming the basis of a new level physical and chemical modification can be established. The possibility of coagulation of magnetic inclusions in the direction of the crystallographic axis C in intercalates is eliminated thanks to the packets of ionic-covalent layers alternate with magnetically active layers. Structures with alternating semiconductor and magnetically active layers are of great interest for spintronics, since they provide the possibility in principle of controlling magnetic properties optically or electrically [1].

Actual interest in nanostructures with alternating semiconductor and magnetically active nanolayers is much wider – for example, spin capacitors and magnetoelectrets. Spin wave can be applicable for unique signal analysis and processing devices owing to their small phase and group velocity, the ease of excitation and reception as well as low propagation losses. In the longer run a quantum coherent spintronic is one of the applications of this work. That is why comprehensive studies of such

structures open up additional possibilities for revealing interesting phenomena and effects that could lead to new directions of their practical application. The above mentioned issues are studied in this work.

2. EXPERIMENT

Synthesis of intercalation compounds Ni_xInSe ($x = 0$; 0.25; 0.5; 0.75; 1.0; 1.25) was carried out by direct synthesis of components in quartz ampoules, pumped out to a pressure of residual gases of 10 Pa. In order to homogenize the alloy, a vibrating pealing was used. As an initial component, substances of the "superpurity" brand were taken. Synthesis was carried out for three days at a temperature below 960 K to prevent the formation of nickel selenides. Further, from synthesized compounds, single crystals were grown using the Bridgman-Stokbarger method.

The rate of the ampoule's immersion was 3 mm/hr with a temperature gradient in the crystal growth zone of 30 deg/cm. For the uniform distribution of impurities in a single crystal and expediting the process of its transition into a solid solution, the grown crystals were thermally treated in pumped quartz ampoules at a temperature of 870 K for 60 hours.

X-ray studies were performed on a Dron-4-07 diffractometer (Cu K_α-irradiation, step 0.05°, range of angle scanning 8-135°). Structural characteristics of Ni_xInSe were calculated by the program "Crysfire" with specification of the parameters by the least squares method.

The temperature dependence of the heat capacity was investigated in the temperature range of 2-300 K using the Quantum Design PPMS-9 device.

Impedance measurements were made in the range of 10^{-3}-10^6 Hz by the instrumentality of the measuring complex "AUTOLAB" of the company "ECO CHEMIE"

(Holland), featuring the computer programs FRA-2 and GPES. The amplitude of the sinusoidal signal applied to the object did not exceed 5 mV. The removal of ambiguous points was carried out by Dirichlet's filter [A, B].

Frequency dependences of the complex impedance Z were analyzed by the graph-analytical method in the ZView 2.3 (Scribner Associates) software package.

The adequacy of the impedance models constructed from the experimental data package was confirmed by the completely random nature of the frequency dependences of the first-order residual differences [2, 3]. Errors of approximation did not exceed 4 %.

3. RESULTS AND DISCUSSION

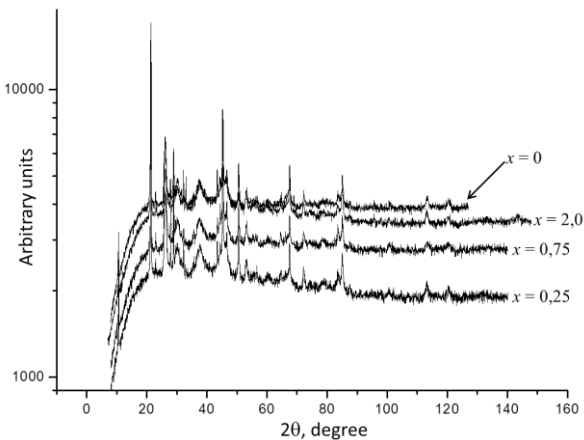The diffraction patterns of pure and the intercalated Ni_xInSe are shown in Fig. 1.

Fig. 1 – The diffraction patterns of Ni_xInSe samples

These structures are indexed in a trigonal system, the spatial group R_3m. X-ray diffraction analysis showed that the obtained material is homogeneous. Neither phases of substitution of nickel selenide compounds nor free nickel Ni_xInSe have been revealed. The absence of diffraction maxima corresponding to the metallic nickel reflects the priority effect of one of the basic structure-forming factors – deformation fields arising in particular from the inconsistency of the permanent lattice constant of the matrix and the intercalant layer. This effect contributes to the formation of discrete nano-islands from the "guest" component, their reproductions with the formation of fractal nets, etc. Thus, during the transition of the crystal to the equilibrium state the atoms of nickel, which with a certain probability could enter the covalent layers of Se-In-In-Se occupy the interlayer space. This is in a good agreement with the theoretical model of "self-purification" proposed in [4].

The concentration dependence of the lattice C parameter is shown in Fig. 2.

As it can be seen, $C(x)$ is nonmonotonic with local minima in the vicinity of values $x = 0.25$ and $x = 0.75$. In general, the distance between the layers decreases in comparison with the original matrix for all investigated values of the degree of nickel guest content. Reduction of the parameter C with the increasing degree of intercalation by $3d$ metals was observed also for dichalcogenides of titanium [5,6].
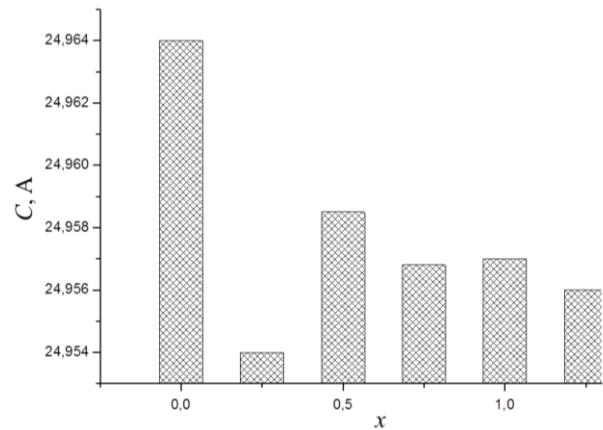

Fig. 2 – Dependence of Ni_xInSe lattice parameter C on nickel concentration x

In the cited sources, this effect is associated with the formation of covalent quasimolecules Me($3d$)-Ti-Me($3d$), which leads to the localization of current carriers in the form of small radius polarons [6]. The non-monotonicity of $C(x)$ indicates the processes associated with the disintegration of covalent quasimolecules, the probable cause of which can be related to a change in the position of the Fermi level, which leads to the Ni-In-In-Ni orbital dehybridization. That all causes the electrons to fill the levels of the nickel atom which resides in the interlayer space leading to the growth of its pushing action on the adjacent layers. Obviously, the effects of "contracting" and "pushing" the crystalline lattice are competitive and in fact they generally determine the nature of the dependence of $C(x)$.

In this perspective, the further reduction of the distance between the layers at $x = 1,25$ is most likely due to the redistribution of the energy topology of the levels in the vicinity of the Fermi level and the reformatting of the system of quasi-molecular bonds. Such processes will necessarily change the kinetics of the electrical current passage, for the interpretation of which the impedance spectroscopy has been applied.

Fig. 3 shows the frequency dependences of the real component of the complex impedance $ReZ(f)$ of the investigated structures for the given temperature.

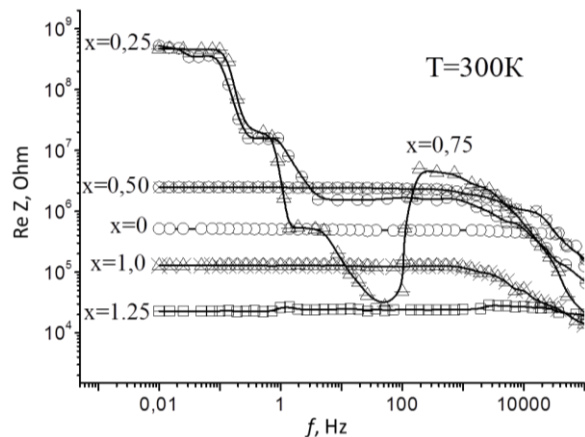**Fig. 3** – Frequency dependences of the real component of the complex specific impedance, perpendicular to the Ni_xInSe layers
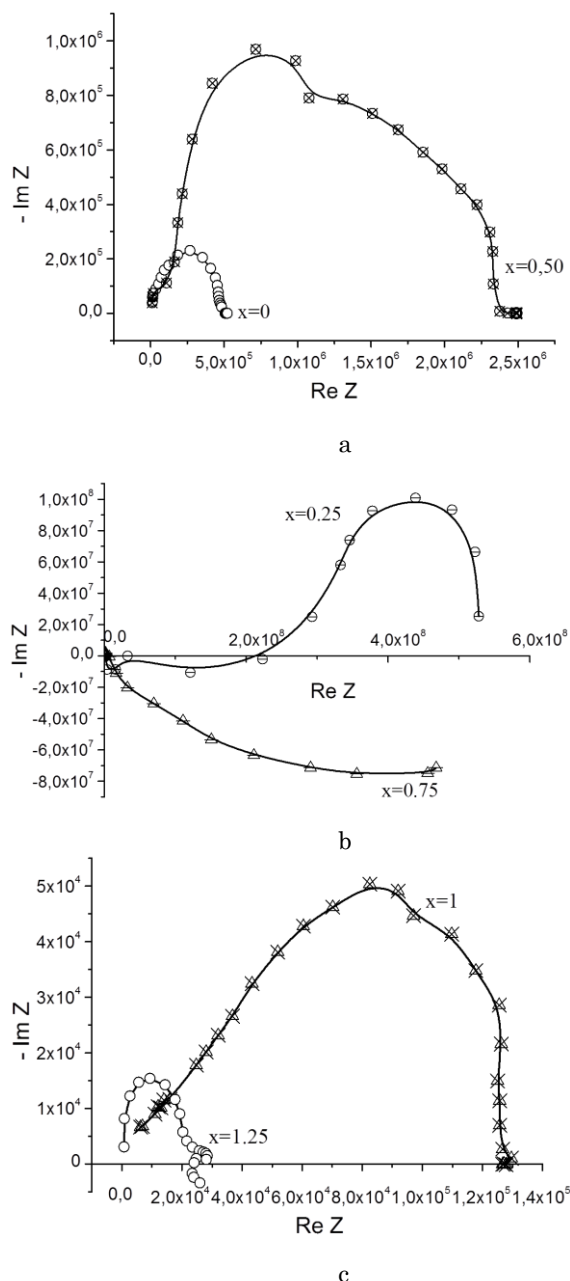
a

b

c

Fig. 4 – Nyquist Diagrams for Ni_xInSe, constructed perpendicular to layers at $x = 0$ and 0.5 (a); $x = 0.25$ and 0.75 (b); $x = 1$ and 1.25 (c)

In order to describe the current-propagation mechanisms in the synthesized intercalates in detail, Nyquist diagrams – the dependence of the imaginary component of the complex impedance on its real component in the plane of the complex impedance are constructed (Fig. 4). It can be seen that for the original matrix ($x = 0$) it has the expected character "one-arc", which reflects the capacitive response of the localized states and the frequency dependent impedance itself, indicating the contribution to the general conductivity of the charge carriers hopping between the localized states, or their excitation in the tail of the density of states or in delocalized zones [7].

After intercalation, the impedance locus is transformed depending on the degree of intercalation. So, for

$x = 0,5$ and $x = 1$, it is a complex curve with a synthetic structure formed by several arcs. This indicates modification of the energy shape of the original matrix of indium selenide by the barriers triggered by guest nickel. But the most peculiar fact was the deformation of low- and medium-frequency branches of $ReZ(f)$ for $x = 0.25$ and $x = 0.75$ (Fig. 3).

Using the method of complex amplitudes it can be shown [12] that the peak values of $ReZ(f)$ can be related to the inductive response of the crystal. The most interesting thing is that with strong deformations of $ReZ(f)$ for $x = 0.75$, the low-frequency branch of the Nyquist diagram practically completely falls into IV-the inductive quadrant of the complex impedance plane. This phenomenon of "negative" capacity is quite well known from literary sources, although its mechanism is not fully investigated and, apparently, has no single nature [9-11].

According to the most general mechanism the inductive behavior occurs even when the charge is introduced into layers of small or superfluous sizes, that is, a range of several nanometers [12]. For $x = 0.25$, the inductive response is observed in the high-frequency region (Fig. 4b), whereas for $x = 1.25$ in the low-frequency one (Fig. 4c). Thus, a good correlation between the nonmonotonicity of the change in the structure of the original matrix, the anomalies in frequency behavior of $ReZ(f)$ and the emergence of a "negative" capacity is observed.

But at the same time, the inductive response at $x = 0.25$; $x = 0.75$ and $x = 1.25$ has a different frequency pattern and, indeed, a different physical nature. The above-described is well illustrated by the temperature dependences of the specific resistance perpendicular to the layers of Ni_xInSe, as shown in Fig. 5.
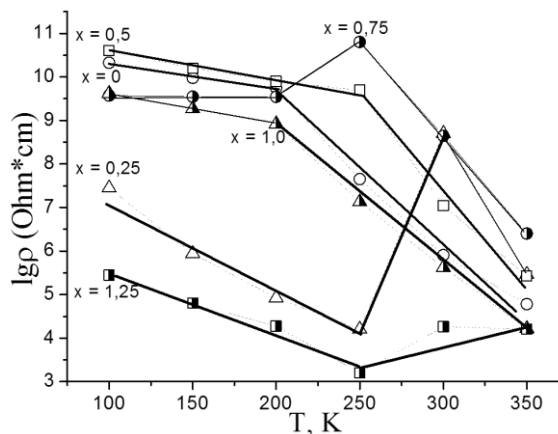

Fig. 5 – Temperature dependences of the specific resistance, perpendicular to the layers for Ni_xInSe

It can be seen that for the indicated values of the guest load ($x = 0.25$; 0.75; 1.25) the temperature genesis of the electrical conductivity differs significantly from both the initial matrix and $Ni_{0,5}InSe$ as well as $Ni_{1,0}InSe$. At the same time, the difference is also well visualized in the processes of current distribution of $Ni_{0.75}InSe$ as compared to $Ni_{0.25}InSe$ and $Ni_{1.25}InSe$, which are characterized by a different nature of the inductive response. This difference consists in the fact that the temperature transition point from the activa-

tion mechanism of conductivity to the non- activation one for $x = 0.75$ is shifted to a low temperature region by 50 K as compared to the one for $x = 0.25$. Moreover, for the latter x value, the activation mechanism at 300 K is characterized by its resumption.

In order to find out the nature of the modification of the electron energy spectrum for nickel intercalated InSe, the temperature dependence of the heat capacity was investigated in [13]. The absence of hysteresis was proved for a temperature range of 2-170 K. For a non-intercalated InSe sample at the lowest temperatures (below 5.5 K), the temperature dependence of the specific heat content is of the order $T^{2.4}$.

The observed deviation from the Debye temperature dependence of T^3 should be expected, since in this case a quasi-twodimensional system with a non-zero interaction between adjacent layers is under investigation.

The temperature dependence of the heat capacity is shown in Fig. 6. As it can be seen from Fig. 6 a linear dependence of heat capacity on T is visualized for this system for a wide temperature range. This unusual fact for semiconductor crystals in this case can definitely be associated with some disordering, which leads to the presence of donor levels near the bottom of the conduction band.

After intercalation with nickel, two following significant changes in temperature dependences of heat capacity $C(T)$ are observed:

- the linear contribution to the thermodynamics of the electrons at the lowest temperatures disappears;

- at temperatures below the Debye temperature, the temperature dependence of the specific heat capacity does not correspond to the expected law of T^{2-3} for quasi-twodimensional systems, nor even to the Debye law T^3, but the dependence $\sim T^{>3}$ is revealed (the power index is greater than 3).
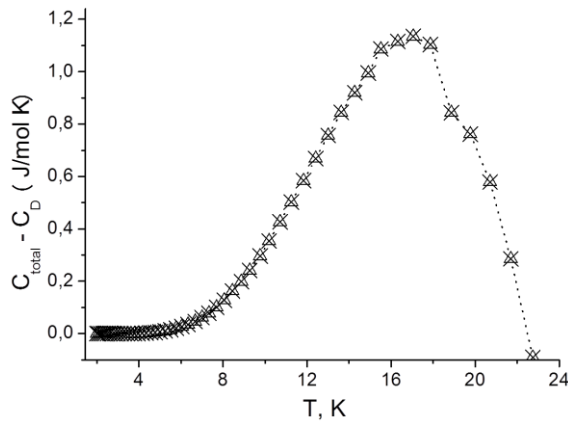

Fig. 6 – The temperature dependence of the difference ($C_{total} - C_D$) for $Ni_{1,0}InSe$

For example, for $x = 1$ this dependence is proportional to $T^{3.2}$ [13]. In this case, even in the extended temperature range up to 12 K, it is well approximated by the function $aT^3 + bT^5$. This enabled to determine Debye temperature of $T_D = 275$ K [13]. T_D is almost invariable with the change in the concentration of the introduced nickel. If the first of the above-mentioned changes in $C(T)$ can be understood on the basis of a change in the position of the Fermi level during inter-

calation, then the other one requires a more detailed analysis. First of all if Debye ($\sim T^3$) heat capacity C_D is subtracted from the total one C_{total}, then, for example, for $x = 1$, the dependence shown in Fig. 6 is obtained.

A sharp non monotonicity of this difference with the maximum in the vicinity of $T = 17$ K is observed. Since for this value of x the contribution of electrons is not noticeable, then this difference (especially in such a wide temperature region) must be linked to the peculiarities of the intercalated lattice. The essence of these peculiarities is that due to the layered structure of the spatial dimensions of the sample itself and its inherent phonon spectrum, they can vary greatly. The application of fractal geometry to describe nano-objects and Euclidean structures with a fractal phonon spectrum has shown [14] that, in the general case, the heat capacity does not necessarily follow the Debye law $C(T) \sim T^3$ even for $T \to 0$. The excessive density of the oscillatory states as compared to the Debye one is inherent to the disordered structures and it can increase, especially at low temperatures [15].

If such nature is characteristic for the studied samples, it should be reflected on the special features of the heat capacity of the guest subsystem, which, according to X-ray data, should be fractalized. To verify this the difference between the heat capacity of the intercalated and nonintercalated samples ($C_{Ni + InSe} - C_{InSe}$) is constructed. Their relative on C_{InSe} values are shown in Fig. 7 [13].
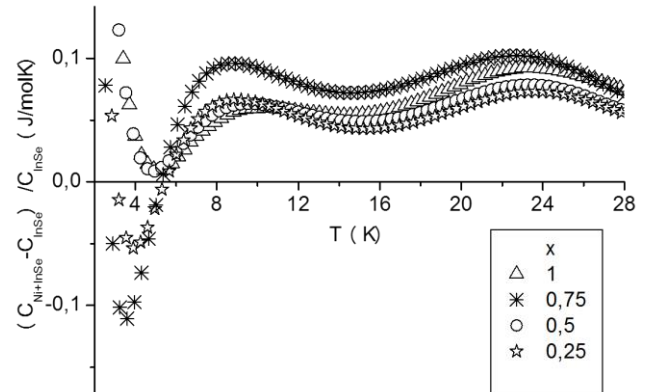

Fig. 7 – Temperature dependences of the normalized difference ($C_{Ni + InSe} - C_{InSe}$)/C_{InSe}

The presence of two maxima in the vicinity of 9 and 24 K is clearly visible. In general, the non-monotonous nature of such dependencies is often associated with the magnetic contribution to the heat capacity at low temperatures in spin and cluster glasses. However, as a rule, such a mechanism is well explained for high-conducting phases where it is accompanied by the growth of the peak of this function with the increasing intercalant load [15].

In our case, this does not work (Fig. 7), so the nature of the maxima at 24 K is unclear. Therefore, taking into an account the out of the ordinary fact that decrease in $C(T)$ of intercalated $Ni_{0.25}InSe$ and $Ni_{0.75}InSe$ crystals as compared to the pure InSe (the function $C_{Ni + InSe} - C_{InSe}$)/C_{InSe} only for these values of x becomes negative in the temperature range 2.89-5.31 K), it should be assumed that the obtained exper-

imental data are most likely to be explained by the change in the fractal structure of the clustered nickel guest subsystem. That in fact provides both an increase and a decrease of $C(T)$ depending on the fractality of the phonon spectrum.

It is possible that the inductive response, which is the most significant for $x = 0.25$ and $x = 0.75$, is due not only to the peculiarities of the electronic structure – the capture of the carriers in quantum wells over the time interval, commensurate with the half-period of the sinusoidal signal, but also due to peculiarities of the fractal structure through the percolation mobility.

4. CONCLUSIONS

1. The formation of discrete nano-islands from the "guest" component that causes their reproduction to form fractal nets is typical for intercalation compounds Ni_xInSe ($x = 0$; 0.25; 0.5; 0.75; 1.0; 1.25).

2. A decrease of the crystal lattice parameter perpendicular to the layers after intercalation is related to the formation of Ni-In-In-Ni quasimolecules, while its

nonmonotonic change with the increasing x is due to the processes of hybridization and de-hybridization of their orbitals.

3. In the synthesized intercalates, an inductive response was found at $x = 0.25$; $x = 0.75$; and $x = 1.25$, which for the indicated values of x has different intensity and frequency manifestation and is conjugated with different electrical pathway patterns and fractal structure of guest content.

4. After intercalation with nickel, the linear contribution to the heat capacity of the electrons at the lowest temperatures disappears, and at temperatures lower than the Debye temperature, the temperature dependence of the specific heat capacity does not correspond to the expected $T^{2 \div 3}$ law for quasi-twodimensional systems, nor even the Debay's law T^3, but the dependence $\sim T^{> 3}$ is revealed.

5. A peculiar decrease in $C(T)$ of intercalated $Ni_{0.25}InSe$ and $Ni_{0.75}InSe$ crystals as compared to the pure InSe can be explained by the change in the fractal structure of the clustered nickel guest subsystem.

REFERENCES

1. B.P. Zarkharchenya, V.L. Korenev, *UFN* **175** No 6, 629 (2005) [in Russian].
2. I. Mora-Sero, J. Bisquert, *Nano Lett.* **6** No 4, 640 (2006).
3. B.O. Seredyuk, R.W. McCullough, H.B. Gilbody *Phys. Rev. A.* **71** 022713 (2005).
4. K.D. Tovstyuk, *Semiconductor materialscience* (K.: Naukova Dumka: 1984).
5. V.G. Pleshchev, N.V. Toporova, A.N. Titov, N.V. Baranov *FTT* **44** No 7, 1153 (2004) [in Russian].
6. A.N. Titov, A.V. Dolgoshein, I.K. Bdikin S.G. Titova, *FTT* **42** No 9, 1567 (2000) [in Russian].
7. N.M. Olekhnovych, I.I. Moroz, A.V. Pushkarev, Yu.V. Radyush, A.N. Salak, N.P. Vyshatko, V.M. Ferreira *FTT* **50** No 3, 472 (2008).
8. N.T. Pokladok, I.I. Grygorchak, O.I. Grygorchak, F.O. Ivashchyshyn, P.Y. Stakhira *Sensor electronics and microsystem technologies* **1(7)** No 4, 69-78 (2010).
9. J. Bisquert, H. Randriamahazaka, G. Garcia-Belmonte, *Electrochimica Acta* **51**, 627 (2005).
10. R.Ya. Shvets, I.I. Grygorchak, A.S. Kurepa, N.T. Pokladoka, Yu.I. Sementsov, G.I. Dovbeshko, Ye. Sheregii, B. Seredyuk, *Acta Physica Polonica A* **128** No 2, 208 (2015).
11. F.O. Ivashchyshyn, I.I. Grygorchak, O.V. Balaban, B.O. Seredyuk, *Mater. Sci. Poland* **35** No 1, 239 (2017).
12. I.I. Grygorchak, S.A. Vojtovych, B.O. Seredyuk, N.K. Tovstyuk, *SEMST* **10** No 4, 81 (2013).
13. A. Baran, M. Botko, M. Kajňaková, A. Feher, *Low Temp. Phys.* **41** No 11, 1191 (2015).
14. V.G. Pleshchev, N.V. Selezneva, V.I. Maksimov, A.V. Korolev, A.V. Podlesnjak, N.V. Baranov *FTT* **51** No 5, 885 (2011) [in Russian].
15. K. Binder, A.P. Young. *Rev. Mod. Phys.* **58**, 801 (1986).